

See discussions, stats, and author profiles for this publication at: <https://www.researchgate.net/publication/259321036>

D14-SCFD3-dependent degradation of D53 regulates strigolactone signaling

Article in *Nature* · December 2013

DOI: 10.1038/nature12878 · Source: PubMed

CITATIONS
522

READS
2,107

35 authors, including:



Feng Zhou
CAS Center for Excellence in Molecular Plant Sciences

11 PUBLICATIONS 1,245 CITATIONS

[SEE PROFILE](#)



Qibing Lin
Chinese Academy of Agricultural Sciences

84 PUBLICATIONS 2,665 CITATIONS

[SEE PROFILE](#)



Yulong Ren
Chinese Academy of Agricultural Sciences

134 PUBLICATIONS 3,451 CITATIONS

[SEE PROFILE](#)



Nitzan Shabek
University of California, Davis

34 PUBLICATIONS 2,063 CITATIONS

[SEE PROFILE](#)

Some of the authors of this publication are also working on these related projects:



cyclic nucleotide-gated ion channels [View project](#)



SYNBIOCHEM [View project](#)

D14-SCF^{D3}-dependent degradation of D53 regulates strigolactone signalling

Feng Zhou^{1,2}, Qibing Lin², Lihong Zhu¹, Yulong Ren², Kunneng Zhou¹, Nitzan Shabek^{3,4}, Fuqing Wu², Haibin Mao^{3,4}, Wei Dong², Lu Gan², Weiwei Ma², He Gao¹, Jun Chen², Chao Yang¹, Dan Wang², Junjie Tan², Xin Zhang², Xiuping Guo², Jiulin Wang², Ling Jiang¹, Xi Liu¹, Weiqi Chen⁵, Jinfang Chu⁵, Cunyu Yan⁵, Kotomi Ueno⁶, Shinsaku Ito⁶, Tadao Asami⁶, Zhijun Cheng², Jie Wang², Cailin Lei², Huqu Zhai², Chuanyin Wu², Haiyang Wang², Ning Zheng^{3,4} & Jianmin Wan^{1,2}

Strigolactones (SLs), a newly discovered class of carotenoid-derived phytohormones, are essential for developmental processes that shape plant architecture and interactions with parasitic weeds and symbiotic arbuscular mycorrhizal fungi. Despite the rapid progress in elucidating the SL biosynthetic pathway, the perception and signalling mechanisms of SL remain poorly understood. Here we show that DWARF 53 (D53) acts as a repressor of SL signalling and that SLs induce its degradation. We find that the rice (*Oryza sativa*) *d53* mutant, which produces an exaggerated number of tillers compared to wild-type plants, is caused by a gain-of-function mutation and is insensitive to exogenous SL treatment. The *D53* gene product shares predicted features with the class I Clp ATPase proteins and can form a complex with the α/β hydrolase protein DWARF 14 (D14) and the F-box protein DWARF 3 (D3), two previously identified signalling components potentially responsible for SL perception. We demonstrate that, in a D14- and D3-dependent manner, SLs induce D53 degradation by the proteasome and abrogate its activity in promoting axillary bud outgrowth. Our combined genetic and biochemical data reveal that D53 acts as a repressor of the SL signalling pathway, whose hormone-induced degradation represents a key molecular link between SL perception and responses.

Shoot branching (tillering in crops) is a major determinant of plant architecture and crop yield, which is under the integrated control of hormonal, developmental and environmental factors^{1–3}. Although the existence of a root-derived transmissible shoot-repressing signal was proposed more than 70 years ago⁴, the identity of this signal(s) has remained elusive. Recent studies with branching mutants in several plant species have demonstrated that SLs, a specific group of terpenoid lactones, are the long-sought branching-repressing hormones, whose function are highly conserved in both monocots and dicots^{5,6}. In addition to repressing shoot branching, SLs also have a role in regulating root growth, leaf senescence and flower development⁷. SLs also act as exogenous signals to promote the symbiosis between land plants and arbuscular mycorrhizal fungi⁸ and stimulate the germination of the parasitic weeds *Striga* and *Orobanche*, which are serious agricultural pests in many parts of the world⁹.

Previous studies have shown that DWARF 3 (D3), *D10*, *D14* (also known as HIGH-TILLERING DWARF 2, HTD2 and *D88*), *D17* (also known as HTD1) and *D27* in rice^{10–14}, MORE AXILLARY GROWTH 1 (*MAX1*), *MAX2*, *MAX3* and *MAX4* in *Arabidopsis*^{15–17}, RAMOSUS 1 (*RMS1*), *RMS4* and *RMS5* in pea¹⁸ and DECREASED APICAL DOMINANCE 1 (*DAD1*), *DAD2* and *DAD3* in petunia^{7,19} are involved in either the biosynthesis or signalling of SLs. Among these genes, *MAX3/RMS5/D17/DAD3*, *MAX4/RMS1/D10/DAD1*, *MAX1* in *Arabidopsis* and *D27* in rice encode the carotenoid cleavage dioxygenase 7 (CCD7), CCD8, CYP711A1 (a cytochrome P450) and a novel β -carotene isomerase, respectively, and are involved in the sequential cleavage of β -carotene and synthesis of SLs²⁰. By contrast, *MAX2/RMS4/D3* and *D14/DAD2*, which encode an F-box protein and a protein of the α/β -hydrolase superfamily, respectively, probably have a role in SL signalling^{12,19,21}.

The structural similarity between MAX2/RMS4/D3 proteins with the auxin receptor TRANSPORT INHIBITOR RESPONSE 1 (TIR1)^{22,23} and jasmonate receptor CORONATINE INSENSITIVE 1 (COI1)²⁴, and D14/DAD2 proteins with the gibberellin receptor GIBBERELLIN INSENSITIVE DWARF 1 (GID1)²⁵, has sparked the speculation that both MAX2/RMS4/D3 and D14/DAD2 could be candidates for the SL receptors²⁶ and that binding and hydrolysis of SLs by D14/DAD2 (refs 19, 27, 28) might be required for triggering proteasome-mediated degradation of an unknown repressor by the Skp1–Cullin–F-box-containing (SCF)^{MAX2} complex^{29,30}. However, the identity of such a repressor and its regulatory mechanisms in SL signalling have remained unknown.

In this study, we identified a gain-of-function rice mutant, *d53*, which displays a SL-insensitive and increased-tillering phenotype. Map-based cloning revealed that *D53* encodes a protein sharing predicted features with the class I Clp ATPase proteins and that it can form a complex with the α/β hydrolase protein D14 and the F-box protein D3. We show that SLs induce D53 degradation by the proteasome–ubiquitin pathway in a D14- and D3-dependent manner. Our studies establish D53 as a repressor of the SL signalling pathway, whose hormone-induced degradation is essential for SL signalling.

***d53* is a rice SL-insensitive mutant**

Previous studies have identified several rice mutants defective in SL biosynthesis or signalling^{10–14}. Because of their highly branched and dwarf phenotype, these mutants were termed ‘*d* mutants’, such as *d3*, *d10*, *d14*, *d17* and *d27*. The rice *d53* mutant³¹ also displayed reduced height and increased tillering, as well as thinner stem and shorter crown root, compared to the wild-type strain (Fig. 1a, b and Extended Data Fig. 1a, b).

¹National Key Laboratory for Crop Genetics and Germplasm Enhancement, Jiangsu Plant Gene Engineering Research Center, Nanjing Agricultural University, Nanjing 210095, China. ²National Key Facility for Crop Gene Resources and Genetic Improvement, Institute of Crop Science, Chinese Academy of Agricultural Sciences, Beijing 100081, China. ³Department of Pharmacology, University of Washington, Seattle, Washington 98195, USA. ⁴Howard Hughes Medical Institute, Box 357280, University of Washington, Seattle, Washington 98195, USA. ⁵National Centre for Plant Gene Research (Beijing), Institute of Genetics and Developmental Biology, Chinese Academy of Sciences, 1-2 Beichen West Road, Beijing 100101, China. ⁶Department of Applied Biological Chemistry, The University of Tokyo, 1-1-1 Yayoi, Bunkyo, Tokyo 113-8657, Japan.

Kinetic analysis showed that at the heading stage, the total tiller number of *d53* was about three times that of the wild type, resulting from an increase in both higher-order and high-node tillers (Fig. 1c and Extended Data Fig. 1c, d). Histological analysis revealed that the sizes of vascular bundles and parenchyma cells in internodes were largely comparable between *d53* and wild-type plants, implying that the shortening and thinning of the *d53* stem were mainly caused by a reduction in cell number (Extended Data Fig. 1e–h). The phenotypes of F₁ heterozygous plants were intermediate between the homozygous parental plants (Extended Data Fig. 2a–g). Genetic analyses of an F₂ population derived from a cross of *d53* and the wild-type parent (Norin 8) showed that the normal, intermediate and dwarf plants segregated as 1:2:1 (33:58:28, $\chi^2 = 0.09$, $P > 0.05$), indicating that the *d53* mutation behaved in a semi-dominant manner (Extended Data Fig. 2h).

The phenotypic similarity between *d53* and the previously reported rice *d* mutants prompted us to examine whether *d53* is defective in SL-mediated inhibition of axillary bud outgrowth. Quantitative PCR with reverse transcription (qRT-PCR) analysis showed that expression of *D10* (encoding CCD8) was similarly upregulated in *d53* (Fig. 1d) as in other *d* mutants, owing to feedback regulation in the SL pathway¹¹. In addition, expression of an inhibitor of axillary bud outgrowth, *FINE CULM 1 (FC1)*³², which is orthologous to the maize *TEOSINTE BRANCHED1 (TB1)*³³ and the *Arabidopsis BRANCHED 1 (BRC1)*³⁴, was also similarly downregulated in the *d53*, *d14* and *d27* mutants (Fig. 1d), suggesting that *D53* is probably involved in SL biosynthesis

or signalling. Moreover, exogenous application of a SL analogue, GR24, effectively inhibited the outgrowth axillary buds of *d27*, but not *d14* or *d53* (Fig. 1e and Extended Data Fig. 3a–c). Further, measurement of SLs produced in the root exudates showed that *d53* accumulated markedly higher levels of 2'-*epi*-5-deoxystrigol (*epi*-5DS), a native SL of rice, than the wild-type cultivar Norin 8 (Fig. 1f). These results indicate that *d53* is a SL-insensitive mutant.

D53 acts as a repressor of SL signalling

D53 was previously mapped to the terminal region of the short arm of rice chromosome 11 (ref. 35). To decipher the molecular defect in *d53*, we isolated *D53* by a map-based cloning approach. Using an F₂ population of ~12,000 plants generated from the cross between Keta Nangka and the mutant, we further delimited the *D53* locus to a 34-kilobase DNA region on the bacterial artificial chromosome (BAC) clone OSJNBBa0032J07, which contains three putative genes (Fig. 2a). Sequence analysis revealed a single-nucleotide substitution and 15-nucleotide deletion in the third exon of LOC_Os11g01330 in *d53*, which resulted in an amino acid substitution (R812T) and deletion of five amino acids (⁸¹³GKTGI⁸¹⁷) (Fig. 2b). To verify that this mutation caused the tillering dwarf phenotype, we generated transgenic plants expressing the wild-type or mutant *D53* gene under the control

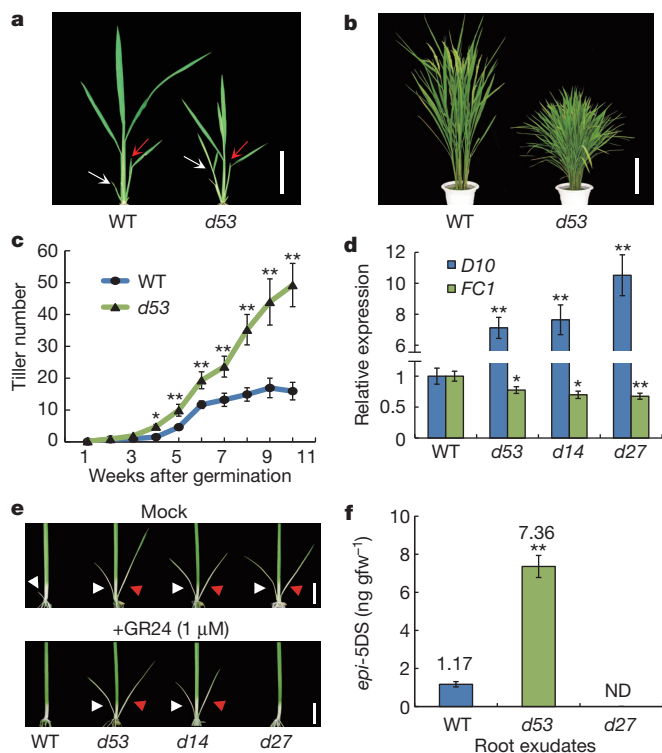


Figure 1 | Phenotype of *d53* mutant. **a, b**, Phenotype of wild type (WT) and *d53* mutant at 4-week-old seedling stage (a) or heading stage (b). White arrows indicate the first tillers in *d53*, which is usually absent in wild type, and red arrows show the second tillers. **c**, Comparison of tillering kinetics at different developmental stages. **d**, qRT-PCR assay showing altered expression of *D10* and *FC1* in *d* mutants. **e**, Responses of rice seedlings to GR24 treatment. Red and white arrowheads indicate the first and second tillers, respectively. **f**, Liquid chromatography-tandem mass spectrometry (LC-MS/MS) measurement of *epi*-5DS levels in root exudates. gfw, per gram fresh weight; ND, not detected. Scale bars, 5 cm (a), 30 cm (b), 2 cm (e). Values are means \pm s.d. (c, $n = 30$ plants; d, f, $n = 3$ replicates). The Student's *t*-test analysis indicates a significant difference (compared with wild type, * $P < 0.05$, ** $P < 0.01$).

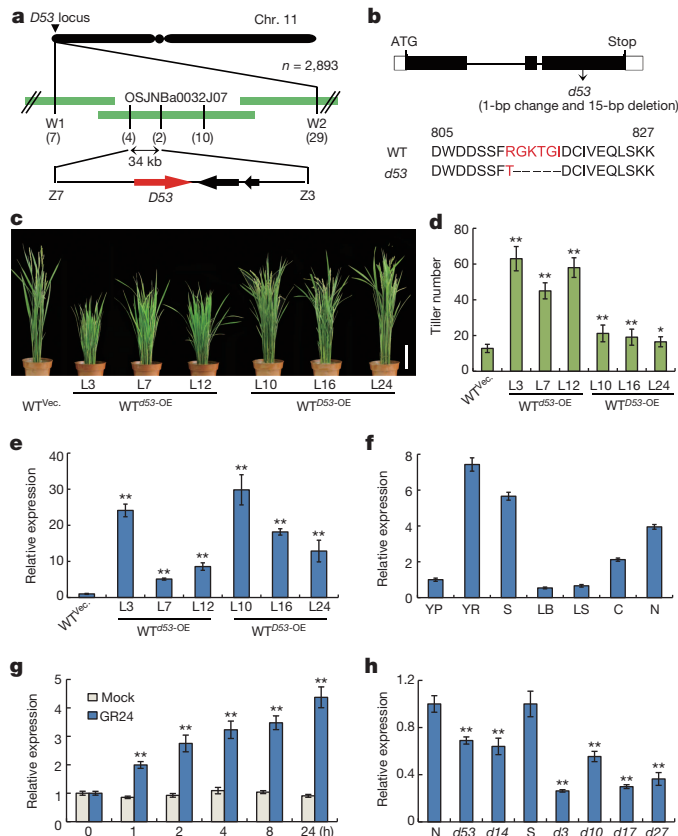


Figure 2 | Map-based cloning and characterization of *D53*. **a**, *D53* was fine-mapped on chromosome 11. The numbers of recombinants are shown in brackets. **b**, Molecular lesions in *d53* mutant. **c**, Phenotypic comparison of *pAct1::D53-GFP* and *pAct1::d53-GFP* transgenic plants. Vector (Vec.), *pAct1::GFP* control. *pAct1::GFP* control. *L*, independent transgenic line. Scale bar, 10 cm. **d**, **e**, Tiller number (d) and relative expression of *D53* (e) of transgenic plants in c. OE, overexpression. **f**, *D53* expression in various organs, including young panicles (YP), young roots (YR), shoots (S), leaf blades (LB), leaf sheaths (LS), culms (C) and nodes (N). **g**, GR24 treatment induces *D53* expression. **h**, Relative expression levels of *D53* in two wild-type varieties Norin 8 (N) and Shioikari (S), and six rice *d* mutants. Each value in d–l represents the mean \pm s.d. (d and f–h, $n = 3$ replicates; e, $n = 20$ plants). The Student's *t*-test analysis indicates a significant difference (compared with control, * $P < 0.05$, ** $P < 0.01$).

of rice *ACTIN 1* promoter (*pAct1*), in a wild-type background. Notably, all transgenic plants expressing the mutant *d53* gene showed a more exaggerated tillering phenotype than those expressing the wild-type *D53* gene. The severity of tillering phenotype in these transgenic plants was correlated with the expression level of the transgene. Notably, over-expression of the wild-type *D53* gene also caused a moderate increase in tillering, compared to the vector control plants (Fig. 2c–e). These observations suggested that the *D53* protein acts as a repressor in the SL-mediated branching-inhibition pathway and that the dominant tillering phenotype of the *d53* mutant was most likely caused by a gain-of-function mutation in *d53*. To further confirm this, we generated *D53* knockdown transgenic plants using an RNA interference (RNAi) approach. As expected, reducing *D53* expression in a *d53* background markedly reduced the tiller number (Extended Data Fig. 3d, e). Taken together, these data support the proposition that the *d53* mutation enhances *D53* activity in repressing SL signalling.

D53 is predicted to encode a protein of 1,131 amino acids. A BLAST search identified a closely related homologue of *D53* (designated *D53*-like, LOC_Os12g01360) with 96.6% amino acid sequence identity in the rice genome. Further, *D53*-like proteins were found in other monocots and dicots, but not in lower plants, animals or microbes, indicating that the *D53*-like clade is specific to higher plants (Extended Data Fig. 4). Sequence analysis by the HHpred structure prediction server revealed that *D53* shares a similar secondary structure composition, despite low primary sequence homology, to proteins of the class I Clp ATPase family, which are characterized by an N-terminal domain, a D1 ATPase domain, an M domain and a D2 ATPase domain³⁶. Notably, the D2 domain of *D53* contains a highly conserved linear sequence, Phe-Asp-Leu-Asn-Leu, which closely matches the ethylene-responsive element binding factor-associated amphiphilic repression (EAR) motif (Extended Data Fig. 5), which is known to interact with the TOPLESS family of proteins and is involved in transcriptional repression³⁷.

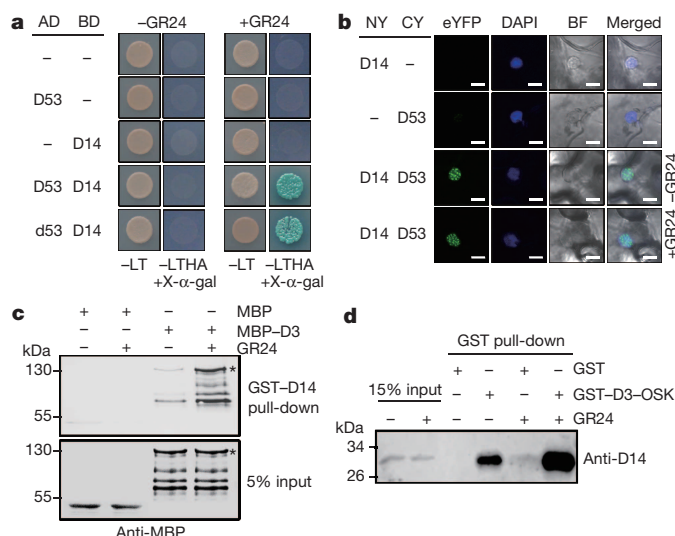


Figure 3 | GR24 promotes the D53-D14 and D14-D3 interaction. **a**, Y2H assay showing that *D53* and *d53* interact with *D14* in the presence of GR24. Yeast transformants were spotted on the control medium (SD –Leu/-Trp (–LT)) and selective medium (SD –Leu/-Trp/-His/-Ade (–LTHA) plus X- α -gal). AD, activating domain; BD, binding domain; SD, synthetic dropout. **b**, BIFC analysis of *D53* and *D14*. The positions of nuclei are indicated by DAPI (4',6-diamidino-2-phenylindole) staining. eYFP, enhanced yellow fluorescent protein. NY and CY stand for the N terminus and C terminus of eYFP, respectively. BF, bright-field image. Scale bars, 10 μ m. **c**, In vitro pull-down assay of recombinant maltose binding protein (MBP)-D3 or MBP using resins containing GST-D14. Asterisks indicate the full-length MBP-D3 protein. **d**, Pull-down assay showing co-immunoprecipitation of *D14* from the *d3* mutant plant extracts, using GST-D3-OSK1 as the bait. ‘Input’ shows that roughly equal amounts of total plant proteins were used.

qPCR analysis revealed that *D53* was widely expressed in the examined rice tissues (Fig. 2f). A *D53*-promoter-driven GUS (β -glucuronidase) reporter gene (*pD53::GUS*) assay showed that GUS staining was observed in the vasculature in roots, shoots, leaves, leaf sheaths, nodes, internodes and young panicles, preferentially in the parenchyma cells surrounding the xylem (Extended Data Fig. 6a–h). Moreover, *D53* expression was upregulated by GR24 treatment in wild-type plants, but downregulated in six *d* mutants, suggesting that expression of *D53* is regulated by SL signalling (Fig. 2g, h). The *D53*-green fluorescent protein (GFP) fusion protein is exclusively localized to the nucleus in rice protoplasts and the *pAct1::D53-GFP* transgenic root cells (Extended Data Fig. 6i–p).

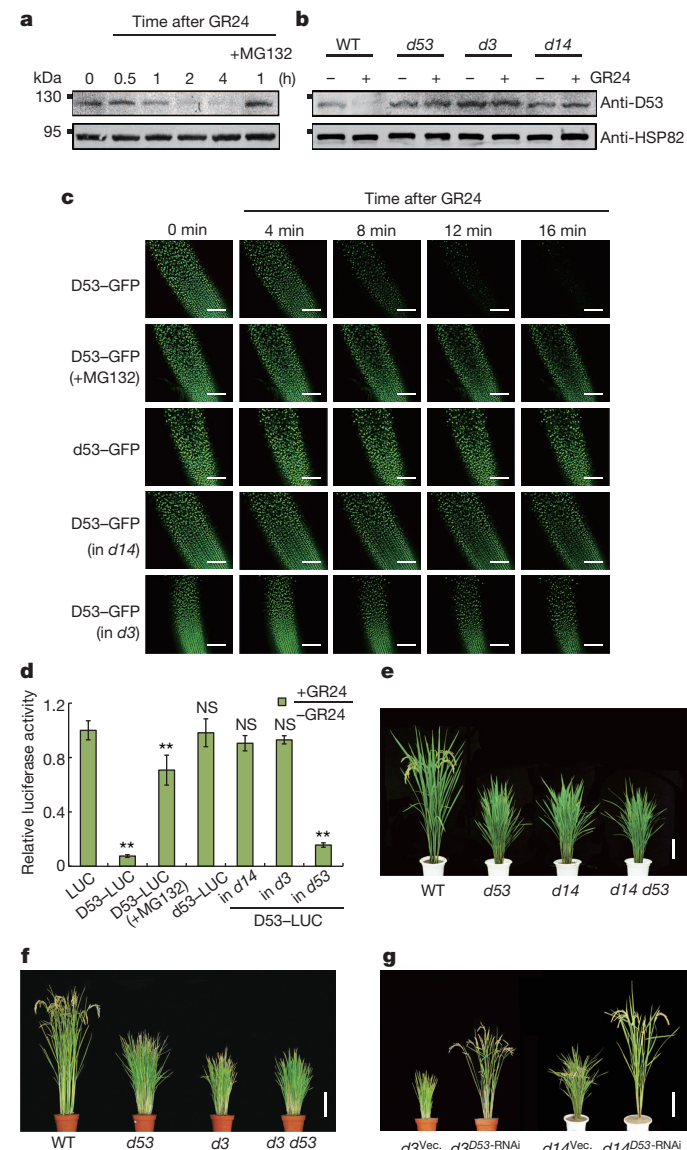


Figure 4 | GR24 promotes D14- and D3-dependent proteasomal degradation of *D53*. **a, b**, Western blot analysis showing that GR24 promotes *D53* protein degradation in wild type (a), but not in *d* mutants (b). 10 μ g of total protein was applied in each lane. **c**, Confocal scanning images showing different degradation patterns of *D53*-GFP and *d53*-GFP fusion proteins in wild-type, *d3* or *d14* backgrounds. **d**, Relative luciferase activity of *D53*-LUC or *d53*-LUC in wild-type, *d14*, *d3* or *d53* protoplasts. Values are means \pm s.d. of three independent experiments. The double asterisks represent significant difference compared with control (LUC) determined by the Student’s *t*-test at $P < 0.01$. NS, not significant. **e, f**, Phenotype of *d14 d53* (e) and *d3 d53* (f) double mutants. **g**, Phenotypes of *D53*-RNAi transgenic plants in *d3* and *d14* backgrounds. Scale bars, 100 μ m (c), 20 cm (e–g).

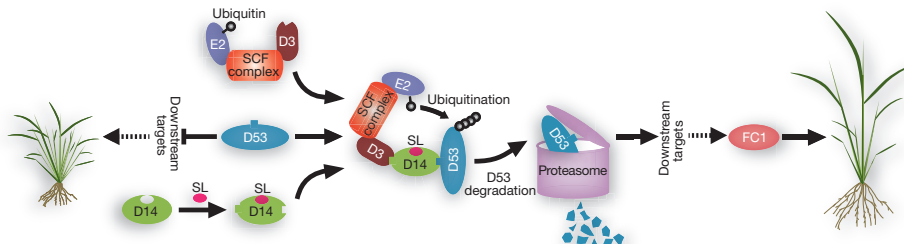


Figure 5 | A schematic model depicting that SL promotes D14-SCF^{D3}-mediated degradation of D53. Bioactive SL binding induces a conformational switch in D14 for SCF^{D3} and D53 binding, which in turn promotes D53 protein

SLs promote D53-D14 and D14-D3 interaction

Previous studies have identified the F-box protein D3 and the α/β hydrolase D14 as two key components of SL signalling in rice^{10,12}, of which D14 and its orthologues in *Arabidopsis* (AtD14) and petunia (DAD2) have been proposed to directly participate in SL perception^{19,27,28}. A yeast two-hybrid (Y2H) assay showed that both D53 and d53 could physically interact with D14 in the presence of GR24 (Fig. 3a). Domain deletion analysis indicated that the D1 domain of D53 was essential for the GR24-dependent D53-D14 interaction. Interestingly, its binding activity was inhibited by the M and D2 domains, although their negative effect can be overcome by the N domain (Extended Data Fig. 7). We verified the D53-D14 interaction in *Nicotiana benthamiana* leaf cell nucleus both in the presence or absence of exogenously applied GR24 using a bimolecular fluorescence complementation (BiFC) assay (Fig. 3b). The observed interaction between D53 and D14 in the absence of exogenously applied GR24 might be due to the effect of endogenous SLs present in the tobacco leaf cells. Consistent with the previously reported GR24-dependent interaction between DAD2 and PhMAX2A (an orthologue of D3 in petunia) in yeast¹⁹, our *in vitro* pull-down assay also revealed a direct physical interaction between D14 and D3 in a GR24-dependent manner (Fig. 3c). Furthermore, using recombinant glutathione S-transferase (GST)-D3-OSK1 fusion protein as the bait, our *in vitro* pull-down assay showed that D14 could be more efficiently co-immunoprecipitated from d3 plant extracts in the presence of exogenously applied GR24 (Fig. 3d). Together, these results suggest that SLs may act to promote complex formation among D14, D3 and D53, linking D53 to the hormone-perception components of the SL signalling pathway.

GR24 promotes D53 protein degradation

To investigate how SL regulates D53, we performed a set of additional experiments. Both western blot analysis and fluorescence microscopy examination showed that GR24 treatment induced rapid degradation of the D53 protein in wild-type cells, but not in d3 or d14 mutant cells (Fig. 4a-c). We further showed that D53 was degraded by the proteasome, as a proteasome inhibitor, MG132, but not other protease inhibitors, effectively blocked GR24-induced D53-GFP degradation (Fig. 4c, d and Extended Data Fig. 8a, b). Notably, unlike the wild-type D53-GFP fusion protein, the mutant d53-GFP fusion protein appeared to be stable in the presence of GR24 (Fig. 4c and Extended Data Fig. 8b). Interestingly, we noted that D53-GFP and D53-luciferase (LUC) were still degraded in the d53 mutant cells, but not in d3 or d14 mutant cells (Fig. 4d and Extended Data Fig. 8c), indicating that the D53 degradation pathway was still operational in the d53 mutant. Together, these results suggest that SL triggers proteasome-mediated degradation of D53 in a D14- and D3-dependent manner. Importantly, the insensitivity of d53 protein to SL-triggered turnover is consistent with the observed dominant gain-of-function mutant phenotype of d53.

To provide genetic support for the functional relationship between D53, D3 and D14, we generated d3 d53 and d14 d53 double mutants. The d3 mutant had more tillers and it was shorter than the d14 and

polyubiquitination. Degradation of D53 protein via the ubiquitin-proteasome pathway leads to expression of SL-responsive genes (such as FC1) and SL responses.

d53 single mutants (Extended Data Fig. 9a). The d14 d53 double mutants exhibited a dwarf tillering phenotype resembling the d14 and d53 parental plants, whereas the d3 d53 double mutant exhibited a dwarf tillering phenotype resembling d3 (Fig. 4e, f and Extended Data Fig. 9a). The lack of obvious additive effects among these mutants suggests that D3, D14 and D53 act in the same signalling pathway. To further test their epistatic relationship, we knocked down D53 gene expression in the d3 and d14 backgrounds. As shown in Fig. 4g and Extended Data Fig. 9b-d, the mutant phenotype of d3 and d14 was restored to nearly wild-type levels, demonstrating that D53 acts downstream of D3 and D14, and that accumulation of D53 protein is responsible for blocking SL signalling and conferring the dwarf tillering phenotype in these mutants.

Discussion

It has been speculated that perception of SLs triggers the degradation of putative repressors by the SCF^{MAX2} ubiquitin ligase complex to suppress shoot branching^{21,29,30}. In this study, we established that D53 acts as a repressor of SL signalling in rice. Consistent with the previous observation of GR24-dependent interaction between DAD2 and PhMAX2A (ref. 19), we found that GR24 also promotes the interaction between D14 with D53 and D3 (Fig. 3). Further, we showed that D53 is targeted for degradation by the proteasome in a D14- and D3-dependent manner (Fig. 4a-d and Extended data Fig. 8). Together, these data collectively support the notion that SL perception by D14 acts to promote ubiquitination of D53 by the D14-SCF^{D3} ubiquitin ligase, and subsequent degradation of D53 by the proteasome, leading to the propagation of SL signal and downstream physiological responses (Fig. 5). Our findings revealed a remarkable similarity between the hormonal perception and signalling mechanism of SL and several other classes of plant hormones, including auxin, jasmonate and gibberellin^{25,38-40}.

Interestingly, a recent study reported that a D53 homologue in *Arabidopsis*, SMAX1, acts downstream of MAX2 (orthologue of rice D3) in repressing the seed germination and seedling photomorphogenesis phenotypes of max2, but not the lateral root formation, axillary shoot growth, or senescence phenotypes of max2 (ref. 41). Further, as observed for D53, three closest homologues of D53 in *Arabidopsis* (designated SMXL6, SMXL7 and SMXL8) were also induced by GR24 treatment⁴¹, suggesting that D53 and its homologues have a broad role in regulating different developmental processes and that the D3/D53 functional module is conserved between monocots and dicots. Consistent with this notion, the SL-analogous compounds known as karrikins also use a MAX2- and KAI2 (D14-LIKE)-dependent pathway to regulate seed germination and seedling growth^{29,42}. The identification and characterization of D53 in SL signalling now sets the stage for further dissection of the mechanisms by which SLs regulate plant form and its complex interactions with parasitic weeds and symbiotic arbuscular mycorrhizal fungi³.

METHODS SUMMARY

The Methods provide detailed information about all experimental procedures, including description of plant materials and growth conditions, map-based cloning of D53, vector construction and plant transformation, rice hydroponic culture

and LC/MS–MS measurement of *epi*-5DS, qRT–PCR, histological analysis and GUS staining, Y2H assay, *in vivo* degradation assay, BiFC assays, recombinant protein preparation, *in vitro* pull-down assays and transient expression assays.

Online Content Any additional Methods, Extended Data display items and Source Data are available in the online version of the paper; references unique to these sections appear only in the online paper.

Received 9 July; accepted 15 November 2013.

Published online 11 December 2013.

- Wang, Y. & Li, J. Branching in rice. *Curr. Opin. Plant Biol.* **14**, 94–99 (2011).
- Domagalska, M. A. & Leyser, O. Signal integration in the control of shoot branching. *Nature Rev. Mol. Cell Biol.* **12**, 211–221 (2011).
- Ruyter-Spira, C., Al-Babili, S., van der Krol, S. & Bouwmeester, H. The biology of strigolactones. *Trends Plant Sci.* **18**, 72–83 (2013).
- Dun, E. A., Brewer, P. B. & Beveridge, C. A. Strigolactones: discovery of the elusive shoot branching hormone. *Trends Plant Sci.* **14**, 364–372 (2009).
- Gomez-Roldan, V. et al. Strigolactone inhibition of shoot branching. *Nature* **455**, 189–194 (2008).
- Umeshara, M. et al. Inhibition of shoot branching by new terpenoid plant hormones. *Nature* **455**, 195–200 (2008).
- Snowden, K. C. et al. The *Decreased apical dominance1/Petunia hybrida CAROTENOID CLEAVAGE DIOXYGENASE8* gene affects branch production and plays a role in leaf senescence, root growth, and flower development. *Plant Cell* **17**, 746–759 (2005).
- Akiyama, K., Matsuzaki, K. & Hayashi, H. Plant sesquiterpenes induce hyphal branching in arbuscular mycorrhizal fungi. *Nature* **435**, 824–827 (2005).
- Cook, C. E., Whichard, L. P., Turner, B., Wall, M. E. & Egley, G. H. Germination of witchweed (*Striga lutea* Lour.): isolation and properties of a potent stimulant. *Science* **154**, 1189–1190 (1966).
- Ishikawa, S. et al. Suppression of tiller bud activity in tillering dwarf mutants of rice. *Plant Cell Physiol.* **46**, 79–86 (2005).
- Arite, T. et al. DWARF10, an *RMS1/MAX4/DAD1* ortholog, controls lateral bud outgrowth in rice. *Plant J.* **51**, 1019–1029 (2007).
- Arite, T. et al. *d14*, a strigolactone-insensitive mutant of rice, shows an accelerated outgrowth of tillers. *Plant Cell Physiol.* **50**, 1416–1424 (2009).
- Zou, J. et al. The rice *HIGH-TILLERING DWARF1* encoding an ortholog of *Arabidopsis MAX3* is required for negative regulation of the outgrowth of axillary buds. *Plant J.* **48**, 687–698 (2006).
- Lin, H. et al. DWARF27, an iron-containing protein required for the biosynthesis of strigolactones, regulates rice tiller bud outgrowth. *Plant Cell* **21**, 1512–1525 (2009).
- Stirnberg, P., van de Sande, K. & Leyser, H. M. O. *MAX1* and *MAX2* control shoot lateral branching in *Arabidopsis*. *Development* **129**, 1131–1141 (2002).
- Booker, J. et al. *MAX3/CCD7* is a carotenoid cleavage dioxygenase required for the synthesis of a novel plant signaling molecule. *Curr. Biol.* **14**, 1232–1238 (2004).
- Sorefan, K. et al. *MAX4* and *RMS1* are orthologous dioxygenase-like genes that regulate shoot branching in *Arabidopsis* and pea. *Genes Dev.* **17**, 1469–1474 (2003).
- Beveridge, C. A. Long-distance signalling and a mutational analysis of branching in pea. *Plant Growth Regul.* **32**, 193–203 (2000).
- Hamiaux, C. et al. *DAD2* is an α/β hydrolase likely to be involved in the perception of the plant branching hormone, strigolactone. *Curr. Biol.* **22**, 2032–2036 (2012).
- Alder, A. et al. The path from β -carotene to carlactone, a strigolactone-like plant hormone. *Science* **335**, 1348–1351 (2012).
- Stirnberg, P., Furner, I. J. & Leyser, H. M. O. *MAX2* participates in an SCF complex which acts locally at the node to suppress shoot branching. *Plant J.* **50**, 80–94 (2007).
- Dharmasiri, N., Dharmasiri, S. & Estelle, M. The F-box protein *TIR1* is an auxin receptor. *Nature* **435**, 441–445 (2005).
- Kepinski, S. & Leyser, O. The *Arabidopsis* F-box protein *TIR1* is an auxin receptor. *Nature* **435**, 446–451 (2005).
- Sheard, L. B. et al. Jasmonate perception by inositol-phosphate-potentiated COI1-JAZ co-receptor. *Nature* **468**, 400–405 (2010).
- Ueguchi-Tanaka, M. et al. *GIBBERELLIN INSENSITIVE DWARF1* encodes a soluble receptor for gibberellin. *Nature* **437**, 693–698 (2005).
- Beveridge, C. A. & Kyozuka, J. New genes in the strigolactone-related shoot branching pathway. *Curr. Opin. Plant Biol.* **13**, 34–39 (2010).
- Zhao, L. H. et al. Crystal structures of two phytohormone signal-transducing α/β hydrolases: karrikin-signaling KAL2 and strigolactone-signaling DWARF14. *Cell Res.* **23**, 436–439 (2013).
- Nakamura, H. et al. Molecular mechanism of strigolactone perception by DWARF14. *Nature Commun.* **4**, 2613 (2013).
- Waters, M. T. et al. Specialisation within the DWARF14 protein family confers distinct responses to karrikins and strigolactones in *Arabidopsis*. *Development* **139**, 1285–1295 (2012).
- de Saint Germain, A., Bonhomme, S., Boyer, F. D. & Rameau, C. Novel insights into strigolactone distribution and signalling. *Curr. Opin. Plant Biol.* **16**, 583–589 (2013).
- Iwata, N., Satoh, H. & Omura, T. Linkage studies in rice. Linkage groups for 6 genes newly described. *Jpn J. Breed.* **27** (suppl.), 250–251 (1977).
- Takeda, T. et al. The *OsTB1* gene negatively regulates lateral branching in rice. *Plant J.* **33**, 513–520 (2003).
- Doebley, J., Stec, A. & Hubbard, L. The evolution of apical dominance in maize. *Nature* **386**, 485–488 (1997).
- Aguilar-Martinez, J. A., Poza-Carrion, C. & Cubas, P. *Arabidopsis BRANCHED1* acts as an integrator of branching signals within axillary buds. *Plant Cell* **19**, 458–472 (2007).
- Wei, L., Xu, J., Li, X., Qian, Q. & Zhu, L. Genetic analysis and mapping of the dominant dwarfing gene *D-53* in rice. *J. Integr. Plant Biol.* **48**, 447–452 (2006).
- Wang, F. et al. Structure and mechanism of the hexameric MeCA-ClpC molecular machine. *Nature* **471**, 331–335 (2011).
- Pauwels, L. et al. NINJA connects the co-repressor TOPLESS to jasmonate signalling. *Nature* **464**, 788–791 (2010).
- Gray, W. M., Kepinski, S., Rouse, D., Leyser, O. & Estelle, M. Auxin regulates SCF^{TIR1}-dependent degradation of AUX/IAA proteins. *Nature* **414**, 271–276 (2001).
- Thines, B. et al. JAZ repressor proteins are targets of the SCF^{COI1} complex during jasmonate signalling. *Nature* **448**, 661–665 (2007).
- Chini, A. et al. The JAZ family of repressors is the missing link in jasmonate signalling. *Nature* **448**, 666–671 (2007).
- Stanga, J. P., Smith, S. M., Briggs, W. R. & Nelson, D. C. *SUPPRESSOR OF MORE AXILLARY GROWTH2* 1 controls seed germination and seedling development in *Arabidopsis*. *Plant Physiol.* **163**, 318–330 (2013).
- Nelson, D. C. et al. F-box protein MAX2 has dual roles in karrikin and strigolactone signalling in *Arabidopsis thaliana*. *Proc. Natl Acad. Sci. USA* **108**, 8897–8902 (2011).

Acknowledgements We thank T. Omura for providing the *d53* mutant, and Z.-Y. Wang and C. Lin for reading of the manuscript. We also thank X. Li for providing the *d3* mutant, W. Liu for providing the *htd2* mutant and I. Takamure for providing the *d10*, *d17* and *d27* mutants. This work was supported by the National Transgenic Science and Technology Program (2011ZX08009-003), 863 National High-tech R&D Program of China (2012AA101100, 2012AA10A301), Jiangsu Province 333 Program (BRA2012126) and National Natural Science Foundation of China (90917017). N.Z. is a Howard Hughes Medical Institute investigator and is supported by the National Science Foundation.

Author Contributions F.Z., L.Z., X.L., Z.C. and H.Z. performed genetic analysis and mapping of *D53*; Q.L., Y.R., N.S., F.W. and H.M. performed the protein interaction experiments; X.Z., X.G. and L.J. performed the genetic transformation; C.W., Jianlin.W., Chao.Y., Jie.W. and C.L. performed the construction and identification of double mutants; K.U., S.I., and T.A. performed the synthesis of *d_e-5DS*; W.C., Jinfang.C., and Cunyu.Y. performed the determination of SLs; K.Z., Y.R. and L.G. performed the degradation experiments; F.Z., H.G. and W.D. performed the Y2H and qRT-PCR experiments; Jun.C., D.W., J.T. and W.M. performed the phenotypic analysis and painted the model picture. Jianmin.W., N.Z. and H.W. directed the project and wrote the manuscript.

Author Information The GenBank accession number for the *D53* nucleotide sequence is KF709434. Reprints and permissions information is available at www.nature.com/reprints. The authors declare no competing financial interests. Readers are welcome to comment on the online version of the paper. Correspondence and requests for materials should be addressed to Jianmin.W. (wanjm@njau.edu.cn or wanjianmin@caas.cn), N.Z. (nzheng@u.washington.edu) or H.W. (wanghaiyang@caas.cn).

METHODS

Plant materials and growth conditions. The wild-type rice (*Oryza sativa* L. subspecies *japonica*) varieties used in this study were Norin 8 (for *d53*, *d14* and *d27*), Akumuro (for *d3*), Shiohari (for *d10* and *d17*) and Kitaake (for transformation analyses). The *d53*-carrying line, KL908, was initially identified from a mutant library of Norin 8 mutagenized by ^{60}Co - γ irradiation³¹. The *d27* and *d14* mutants were described previously^{14,43}. The *d3* mutant used in this work carries a premature stop codon (unpublished data). The *d14 d53* and *d3 d53* double mutants were generated by crossing their respective parental lines and identified by genotyping from their respective F₂ or F₃ populations.

Rice plants were cultivated in the experimental field at the Nanjing Agricultural University in Nanjing in the natural growing seasons. For qRT-PCR, GR24 treatment, SL analyses and transient expression assay, the seedlings of wild-type and mutants were grown in climate chambers (HP1500GS, Ruihua) at 70% humidity, under long-day conditions with daily cycles of 14 h of light at 30 °C and 10 h of dark at 25 °C. Light was provided by fluorescent white-light tubes (400–700 nm, 250 $\mu\text{mol m}^{-2} \text{s}^{-1}$).

Map-based cloning of *D53*. To map the *D53* locus, the *d53* mutant was crossed with a polymorphic *javanica* variety, Ketan Nangka. Rough mapping was performed with simple sequence repeat (SSR) markers W1 (5'-GGATGATGAGA TCCTAATGTAGAA-3' and 5'-CATCCITGGAAAATAGTGGG-3') and W2 (5'-GGCTTCATCTTGGCGACC-3' and 5'-CCGGATTACGAGATAAACT CTC-3') using 242 normal plants obtained in the F₂ population. Using 2,893 normal plants, *D53* was finally mapped to a region between the SSR marker Z7 (5'-C AGAGACCAAAGAACAGAG-3' and 5'-GGAGACGTGTGAGCTACAAC-3') and a derived cleaved amplified polymorphic sequence (dCAPS) marker Z3 (5'-G TTACCGCTCCTCCTCAGC-3' and 5'-AGTAAAATGTGGAGGGGCA-3').

Vector construction and plant transformation. To generate the *pAct1::D53-GFP* and *pAct1::d53-GFP* constructs, full-length complementary DNAs (cDNAs) of *D53* and *d53* were amplified, and the PCR products were then cloned into the binary vector AHLG⁴⁴ using the In-Fusion Advantage PCR Cloning Kit (Clontech) and sequenced (Biomed). The *pAct1::GFP*, *pAct1::D53-GFP* and *pAct1::d53-GFP* constructs were introduced into the wild-type variety Kitaake. The *pAct1::D53-GFP* transgene was introduced into *d3* and *d14* backgrounds by genetic crosses.

To knock down the *D53* gene, the *D53*-RNA interference (*D53*-RNAi) vector was constructed using a 475-base pair cDNA fragment. The PCR fragment was cloned into the pEASY-Blunt cloning vector (TransGen), and the gene-specific fragment was prepared by double digestion with KpnI-SacI and PstI-BamHI, respectively, and then the PCR products were ligated to both sides of the *FAD2* intron in the binary vector pCubi1390- Δ *FAD2* in opposite orientation⁴⁵ and sequenced. The resultant constructs *D53*-RNAi and the control vector pCubi1390- Δ *FAD2* were separately introduced into *d53*, *d3* and *d14* mutants.

To analyse the expression pattern of the *D53* gene, a 2.7-kilobase promoter fragment was cloned into the binary vector pCAMBIA-1381Z and sequenced to create the *pD53::GUS* reporter gene construct, which was then introduced into wild-type rice cultivar Norin 8. All transgenic rice plants were generated using *Agrobacterium*-mediated transformation of rice calli, as described previously⁴⁶. **Rice hydroponic culture and LC/MS-MS analysis of *epi*-5DS.** Preparation of hydroponic culture solution and treatment with GR24 (<http://www.chiralix.com/>) were performed as described previously⁶. In brief, surface-sterilized rice seeds were incubated in sterile water at 30 °C in the dark for 2 days. The germinated seeds were transferred into hydroponic culture medium solidified with 0.5% agar and cultured at 30 °C for 5 days. The 1-week-old seedlings were then transferred to a plastic pot containing hydroponic culture solution (500 ml) and grown for an additional 7 days (total 2 weeks) or 28 days (total 5 weeks). The hydroponic culture solution with or without 1 μM GR24 was renewed every week. For SL analysis, the 1-week-old seedlings were grown in hydroponic culture medium without P_i for an additional 14 days (total 3 weeks).

SL analysis in rice root exudates was performed according to a previously described method¹⁴ with minor modifications. For each sample, the weight of fresh rice roots was recorded and 50 ml hydroponic culture medium was loaded onto a pre-equilibrated Oasis HLB 3cc cartridges (Waters) after adding 1 ng d₆-5DS as the internal standard. Subsequently, the columns were washed with de-ionized water. The SL-containing fraction, eluted with acetone, was collected and dried up under nitrogen gas, then reconstructed in acetonitrile and subjected to UPLC-MS/MS analysis. The UPLC-MS/MS system consists of a triple quadrupole tandem mass spectrometer (Quattro Premier XE; Waters MS Technology) and an Acquity Ultra Performance Liquid Chromatograph (Acquity UPLC; Waters) equipped with a reverse phase column (BEH-C18, 2.1 × 100 mm, 1.7 μm ; Waters). Mobile phase A (99.95% H₂O + 0.05% acetic acid) and mobile phase B (99.95% ACN + 0.05% acetic acid) were pumped at a rate of 0.4 ml min⁻¹. The gradient started with 50% A and increased B from 50% to 70% in 5 min. The column temperature was set to 25 °C. MS parameters were set to the following values: desolvation gas flow,

800 L h⁻¹; capillary voltage, 3.8 kV; cone voltage, 24 V; desolvation temperature, 350 °C; source temperature, 110 °C; collision energy 14 V, using multiple reaction monitoring (MRM) transition of *m/z* 331 > 216 for the *epi*-5DS detection, and MRM transition of *m/z* 337 > 222 for the d₆-5DS detection. Data were analysed with MassLynx software (V.4.1). The *epi*-5DS concentrations of rice exudates were calculated by comparing the MRM relative response of *epi*-5DS with the d₆-5DS ones then divided by the weight of fresh rice roots.

qRT-PCR. Total RNA was extracted using the RNeasy Plant Mini Kit (QIAGEN). Then, 20 μl cDNA was synthesized using 1 μg RNA with the QuantiTect Reverse Transcription Kit (QIAGEN). qRT-PCR (20 μl reaction volume) was carried out using 0.5 μl cDNA, 0.2 μM of each gene-specific primer and SYBR Premix Ex Taq Kit (TaKaRa) in an ABI PRISM 7900HT (Applied Biosystems) according to the manufacturer's instructions. The rice ubiquitin gene was used as the internal control. The gene-specific primers used for qRT-PCR are: ubiquitin gene (LOC_Os03g13170) (5'-AACAGCTGAGGCCAAGA-3' and 5'-ACGATTGATTAACCAGTCCA TGA-3'); *D53* gene (5'-CCAAGCAGTTGAAGCGAC-3' and 5'-CCGCAAGTT TATCAAAGTCAA-3'); *D10* gene (5'-CGTGGCGATATCGATGGT-3' and 5'-CG ACCTCCTCGAACGTCIT-3'); *FC1* gene (5'-CGACAGCGGCAGCTACTAC-3' and 5'-GCGAATTGGCGTAGACGA-3'). Data from three replicates were analysed following the relative quantification method⁴⁷.

Histological analysis and GUS staining. Culm segments of rice were fixed in FAA (formalin/acetic acid/50% ethanol, 2:1:17 (v/v)) overnight, followed by a series of dehydration and infiltration, and embedded in paraffin (Paraplast Plus; Sigma-Aldrich). The tissues were sliced into 8–12- μm sections with a microtome (Leica RM2265), and affixed to microscope slides. Paraffin was removed from the sections using xylene, and the sections were dehydrated through a gradient ethanol series, and stained with toluidine blue. Sections were viewed under a light microscope (Leica DM5000B) and photographed using a Micro Colour charge-coupled device camera (Leica DFC490).

GUS histochemical staining was performed according to a method described previously⁴⁸. Various tissues or hand-cut sections of *pD53::GUS* T₁ generation transgenic plants were incubated in a staining solution containing 100 mM NaPO₄ buffer, pH 7.0, 2 mM X-Gluc, 0.5 mM K₃Fe(CN)₆, 0.5 mM K₄Fe(CN)₆, 0.1% Triton X-100 and 10 mM Na₂-EDTA at 37 °C. Samples were vacuum-infiltrated briefly at the initiation of staining with X-Gluc solution. After staining, the staining solution was removed and the sample was washed with several changes of 50% ethanol until the tissue became clear. Images were taken directly or under the stereomicroscope.

Y2H assay. Coding regions of the rice *D53*, *d53* and various domain deletion variants of *D53* were cloned into the Y2H 'prey' vector pGADT7 (Clontech). The coding region of rice *D14* was cloned into the Y2H 'bait' vector pGBT7 (Clontech). Bait and prey constructs were co-transformed into the yeast (*Saccharomyces cerevisiae*) strain Y2HGold (Clontech) and the resultant yeast stains were grown on SD – Leu/– Trp plates for 3 days at 30 °C. Interactions between bait and prey were examined on the control media – LT (SD – Leu/– Trp) and selective media – LTHA (SD – Leu/– Trp/– His/– Ade) or – LTHA plus X- α -gal in the presence or absence of 5 μM GR24. Plates were incubated for 4 days at 30 °C. Yeast strains containing *D53*, *d53* or *D14* in combination with pGADT7 or pGBT7 were used as controls.

Antibody preparation. For detection of *D53*, a His-fused protein-specific polypeptide (amino acids 963–1,112 of *D53* protein) was expressed in BMRosetta (DE3) cells (Biomed), and then affinity purified. Subsequently, the recombination protein was injected into rabbits to produce polyclonal antibodies against *D53* (Abmart). For detection of *D14* protein, a His-fused polypeptide (amino acids 153–302 of *D14*) was expressed in BMRosetta (DE3) cells. Purified fusion protein was injected into rats to produce polyclonal antibodies against *D14* (Abmart). The loading control used is anti-HSP82 antibody (Beijing Protein Innovation).

In vivo degradation assay of *D53*. One-week-old rice seedlings were treated with or without 5 μM GR24 and collected at different time points. To block proteasomal protein degradation, seedlings were pre-treated with 40 μM MG132 for 2 h. Total protein was extracted and denatured in the SDS sample buffer containing 5% β -mercaptoethanol (β -ME) at 95 °C for 10 min. Western blots were performed using the antiserum against *D53* and visualized by an enhanced horseradish peroxidase-diaminobenzidine (HRP-DAB) substrate kit (Tiangen).

The *pAct1::D53-GFP* and *pAct1::d53-GFP* transgenic plants were treated with 5 μM GR24 with or without the following inhibitors: MG132 (40 μM), AEBSF (500 μM), pepstatin A (1 μM) or leupeptin (20 μM). GFP fluorescence in nuclei of transgenic root cells was observed and imaged with a Zeiss LSM 700 laser scanning confocal microscope.

BiFC assay. The full-length *D14* and *D53* cDNAs were cloned into the binary vectors pSPYNE173 and pSPYCE(M) to create the *D14-NY* and *D53-CY* vectors, respectively. For transient expression, *A. tumefaciens* strain EHA105 carrying the gene of interest (at an *OD*₆₀₀ of 0.1) was co-infiltrated with p19 strain into a 5-week-old *N. benthamiana* leaf as described previously⁴⁹. After 2 days, infiltrated leaves were sprayed with (+) or without (–) 5 μM GR24 24 h before leaf excision. The

eYFP and DAPI fluorescent signals of the infiltrated leaves were monitored sequentially using a laser confocal scanning microscope. The wavelengths for eYFP and DAPI were 514 and 405 nm for excitation, and 527 and 488 nm for detection, respectively.

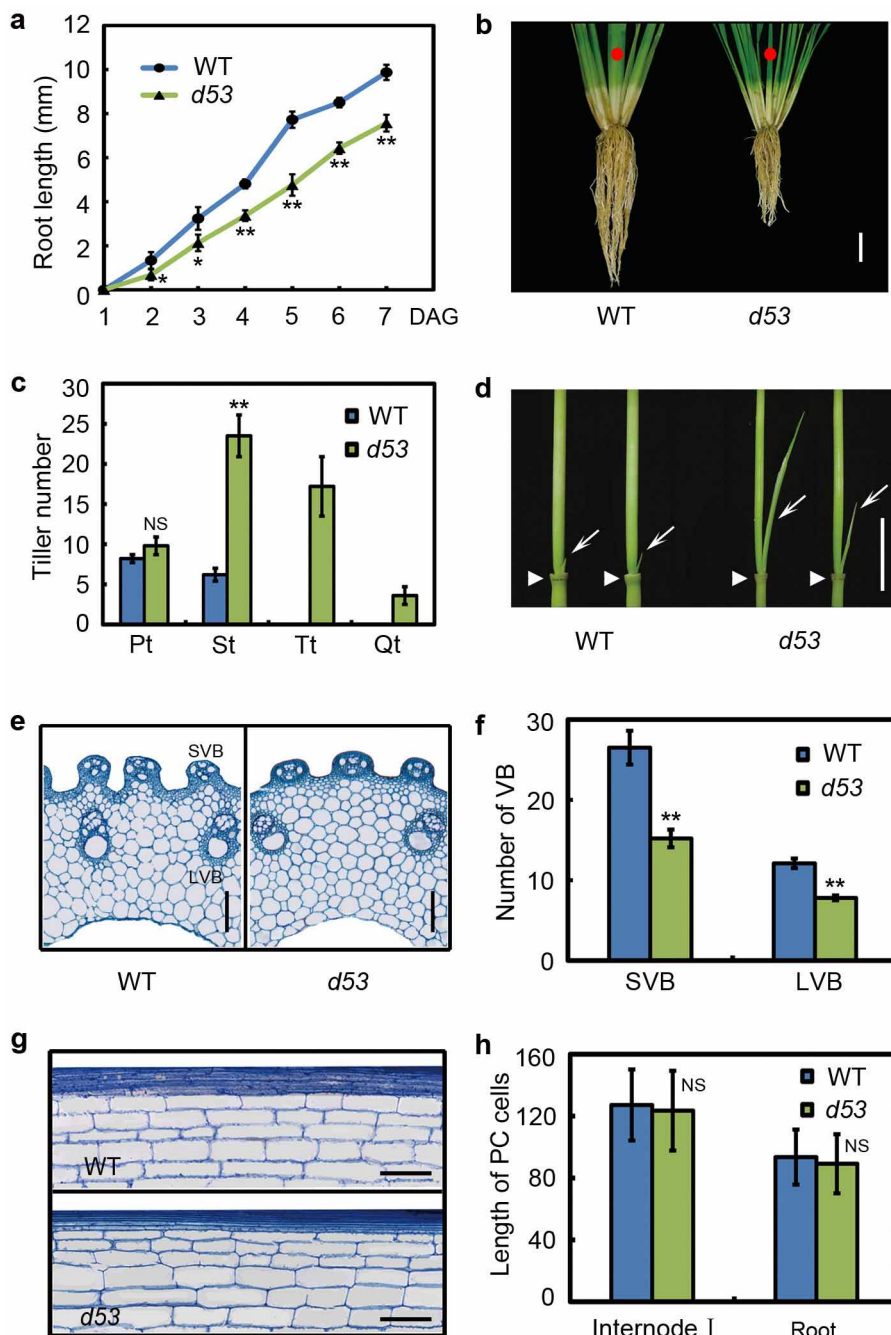
Recombinant protein preparation. The full-length open reading frames of D3-OSK1 and D14 were cloned into the pGEX4T-1 vector, generating a fusion with the GST protein. The full-length cDNA of D3 was cloned into the pMAL-c2x vector to generate a fusion with MBP. Expression of GST, GST-D3-OSK1, GST-D14, MBP and MBP-D3 in BL21 Rosetta cells was induced with 0.1 mM isopropyl- β -D-thiogalactoside at 20 °C for 16 h. Fusion proteins were purified using GST Bind Resin (Novagen) or amylose-affinity chromatography (New England Biolabs) according to the manufacturer's protocols and quantified by the Bio-Rad protein assay reagent.

Pull-down assays. One-week-old rice seedlings were pre-treated with 40 μ M MG132 for 1 h and then treated with or without 5 μ M GR24 for 30 min. Total proteins were subsequently extracted in a radioimmunoprecipitation assay (RIPA) buffer (50 mM Tris-HCl, pH 7.2, 150 mM NaCl, 10 mM MgCl₂, 1 × complete protease inhibitor cocktail, Roche) containing 40 μ M MG132. After centrifugation (16,000g at 4 °C), the supernatant was collected. Total protein concentration was determined by the Bradford protein assay kit (Bio-Rad). Roughly equal amounts of purified GST and GST-D3-OSK1 fusion proteins (about 50 μ g) were affixed to GST Bind Resin and then mixed with 300 μ l of plant extract (containing 1.5 mg total proteins). After being gently shaken at 25 °C for 15 min, the resin was washed five times with RIPA buffer. During all the procedures, 5 μ M GR24 was added to the assay mixture for GR24-treated seedlings and was not added to the protein samples from seedlings not treated with GR24. Proteins were detected with anti-D14 antibodies at 1:1,000 dilution and visualized with enhanced chemiluminescence reagent (GE Healthcare).

For *in vitro* pull-down, GST-D14 (5 μ g) was incubated with MBP-D3 (6 μ g) or MBP (2 μ g) at 25 °C for 15 min in 300 μ l of binding buffer (20 mM Tris-HCl, pH 7.6, 2.5 mM β -ME and 0.1 M NaCl) with or without 10 μ M GR24. After incubation, 20 μ l of GST resin was added. After further incubation at 25 °C for 15 min, the resin was washed five times with the washing buffer (20 mM Tris-HCl, pH 7.5, 500 mM NaCl and 0.5% Triton X-100). The washing buffer also contains 10 μ M GR24 where appropriate. After washing, 40 μ l of 1 × SDS-PAGE sample buffer were added, the mixture was denatured, and the sample was loaded on a 8% SDS-PAGE gel, and proteins were detected by the HRP-conjugated anti-MBP antibody (New England Biolabs) and visualized with enhanced chemiluminescence reagent (GE Healthcare).

Transient expression assays. The *D53*, *d53*, *D3* and *D14* full-length cDNAs were cloned into the vector pA7-GFP or pGreenII 0800-LUC to generate D53-GFP or D53-LUC recombinant plasmids for transient expression assays, respectively. Plasmids DNA was prepared using the Plasmid Midi Kits (Qiagen) according to the manufacturer's instructions. For preparation of rice protoplasts, the sterilized seeds were germinated and grown in climate chambers for 7–10 days. Green tissues from the stem and sheath of 40–60 rice seedlings were used. The protoplasts isolation and polyethyleneglycol (PEG)-mediated transfections procedure were carried out as described previously⁵⁰. GFP fluorescence from protoplasts was observed and imaged as described above. For measurement of the relative luciferase activity, protoplasts were incubated overnight and then treated with or without 5 μ M GR24 for 4 h. For MG132 treatment, 40 μ M MG132 was added to the sample and incubated for 1 h before addition of GR24. Activities of firefly luciferase (fLUC) and Renilla luciferase (rLUC) were determined with the Dual-Glo Luciferase Assay System (Promega). The data were represented as the ratio of fLUC/rLUC activity.

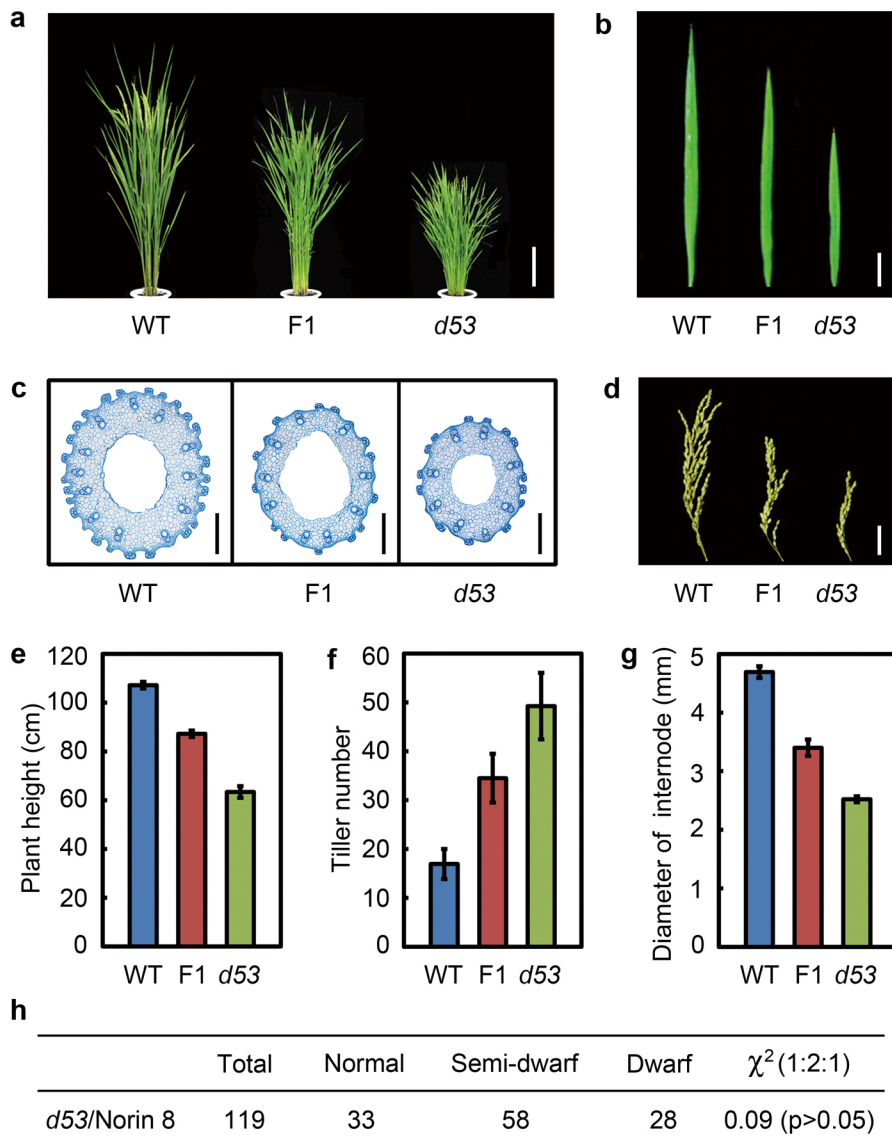
43. Liu, W. et al. Identification and characterization of *HTD2*: a novel gene negatively regulating tiller bud outgrowth in rice. *Planta* **230**, 649–658 (2009).
44. Itoh, H., Ueguchi-Tanaka, M., Sato, Y., Ashikari, M. & Matsuoka, M. The gibberellin signaling pathway is regulated by the appearance and disappearance of SLENDER RICE1 in nuclei. *Plant Cell* **14**, 57–70 (2002).
45. Zhou, K. et al. *Young Leaf Chlorosis 1*, a chloroplast-localized gene required for chlorophyll and lutein accumulation during early leaf development in rice. *Planta* **237**, 279–292 (2013).
46. Hiei, Y., Ohta, S., Komari, T. & Kumashiro, T. Efficient transformation of rice (*Oryza sativa* L.) mediated by *Agrobacterium* and sequence analysis of the boundaries of the T-DNA. *Plant J.* **6**, 271–282 (1994).
47. Livak, K. J. & Schmittgen, T. D. Analysis of relative gene expression data using real-time quantitative PCR and the $2^{-\Delta\Delta C_T}$ method. *Methods* **25**, 402–408 (2001).
48. Jefferson, R. A., Kavanagh, T. A. & Bevan, M. W. GUS fusions: β -glucuronidase as a sensitive and versatile gene fusion marker in higher plants. *EMBO J.* **6**, 3901–3907 (1987).
49. Waadt, R. et al. Multicolor bimolecular fluorescence complementation reveals simultaneous formation of alternative CBL/CIPK complexes in planta. *Plant J.* **56**, 505–516 (2008).
50. Zhang, Y. et al. A highly efficient rice green tissue protoplast system for transient gene expression and studying light/chloroplast-related processes. *Plant Methods* **7**, 30 (2011).



Extended Data Figure 1 | Phenotypes of *d53* mutant. **a**, Comparison of crown root growth in wild-type (WT) and *d53* mutant. DAG, days after germination. Each value represents the mean \pm s.d. of 25 seedlings. **b**, Root phenotype of 7-week-old wild type and *d53* at the tillering stage. Red dots indicate the main culms. **c**, Comparison of different types of tillers between wild type and *d53* at the heading stage. Pt, primary tillers; St, secondary tillers; Tt, tertiary tillers; Qt, quaternary tillers. Each value represents the mean \pm s.d. of 20 seedlings. **d**, Morphology comparison of tiller buds at the second node between wild type and *d53*. White arrows and arrowheads indicate the tiller buds and the second nodes, respectively. **e**, Transverse sections of the first

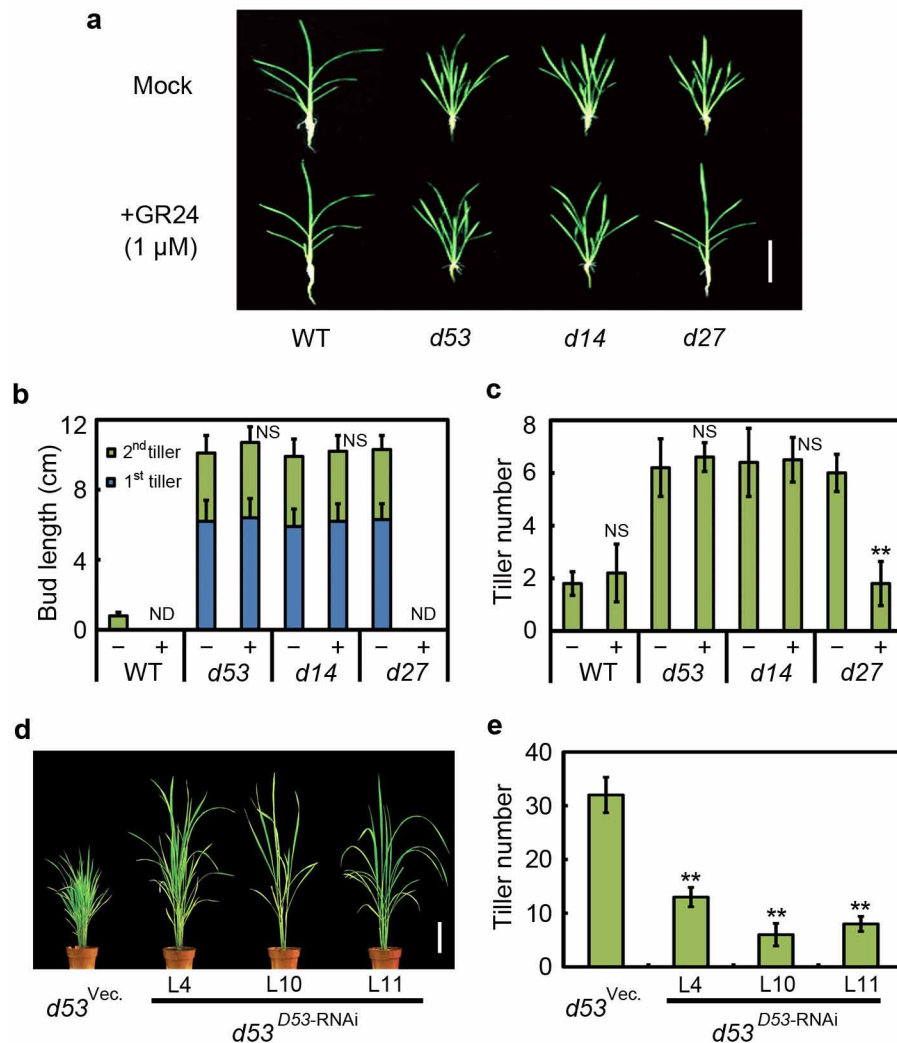
internode of wild type and *d53*. **f**, Number of vascular bundles (VB) calculated from transverse sections of the first internode of wild type and *d53*. SVB, small vascular bundle; LVB, large vascular bundle. Data are means \pm s.d. ($n = 10$).

g, Longitudinal sections of the first internode of wild type and *d53*. **h**, Comparison of parenchyma (PC) cell length in first internode and root between wild type and *d53*. Data are means \pm s.d. ($n = 10$). Differences with respect to the wild type that were found to be significant in a *t*-test are indicated with asterisks (* $P < 0.05$; ** $P < 0.01$; NS, not significant). Scale bars, 10 cm (b), 2 cm (d), 100 μ m (e, g).



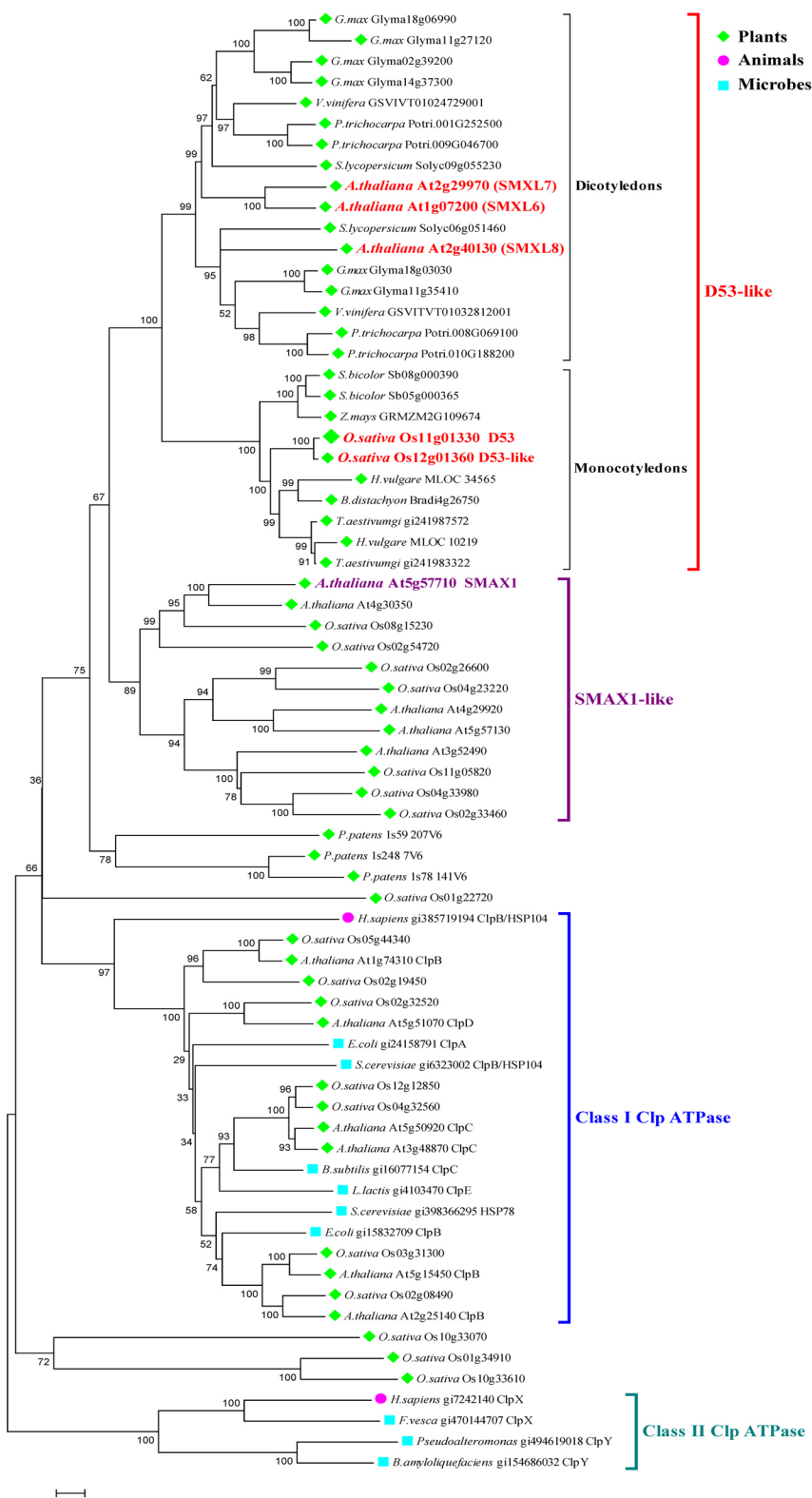
Extended Data Figure 2 | *d53* mutation behaves in a semi-dominant manner. **a, b,** Comparison of wild type, heterozygous (F_1) and homozygous *d53* plants at the heading stage (**a**), flag leaf (**b**), cross section of the first internode (**c**), panicle (**d**), plant height (**e**), tiller number (**f**) and diameter of the

third internode (**g**). Scale bars, 20 cm (**a**, **d**) and 500 μ m (**c**). For **e–g**, each value represents the mean \pm s.d. ($n = 25$). **h**, Segregation of F_2 progeny from a self-pollinated F_1 plant (*d53* \times Norin 8).



Extended Data Figure 3 | *d53* is insensitive to GR24 treatment and confers enhanced tillering-promoting activity. **a**, Response of 5-week-old wild type, *d53*, *d14* and *d27* to the application of 1 µM GR24. **b**, Tiller bud length of 2-week-old wild type, *d53*, *d14* and *d27* seedling treated with (+) or without (−) 1 µM GR24. Data are means ± s.d. (*n* = 10). ND, not detected. **c**, Numbers of tillers showing outgrowth (>2 mm) for 5-week-old wild type, *d53*, *d14* and *d27* plants treated with (+) or without (−) 1 µM GR24. Data are means ± s.d. (*n* = 10). Asterisks in **c** denote significant differences between treated and

untreated samples within the same genotype (two tailed Mann–Whitney *U* test, *P* < 0.01; NS, not significant). **d**, *D53* RNAi transgenic plants exhibit reduced tillering in the *d53* mutant background. *d53*^{Vec.}, *d53* transformed with the pCUBi1390-^ΔFAD2 control. **e**, Tiller number of RNAi transgenic lines in **d** at the tillering stage. Each value represents the mean ± s.d. of six plants (*T*₁ generation). L4, L10 and L11 represent three independent lines. The *t*-test analysis indicated a significant difference (compared with vector control, ***P* < 0.01). Scale bars, 20 cm (**a**), 10 cm (**d**).

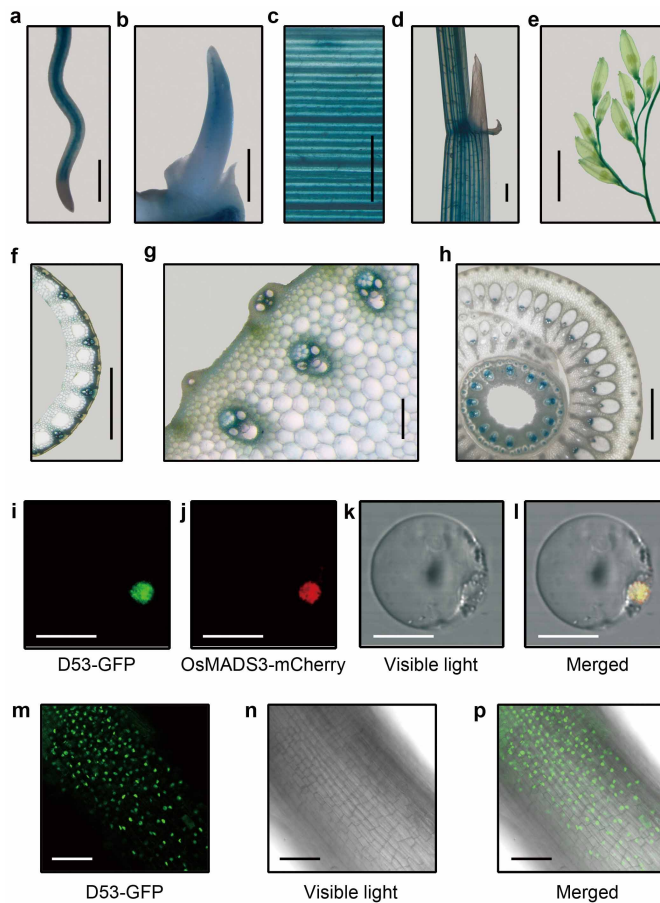


Extended Data Figure 4 | Phylogenetic analysis of D53 protein. Using the D53 protein sequence as the query in tBLASTn searches, homologues were identified from different organisms with a permissive cutoff E value of 1×10^{-3} . The sequences chosen from representative genomes were aligned

and used to generate the neighbour-joining phylogenetic tree with 1,000 bootstrap replicates. The clade names were given on the basis of known sequences in each clade, which is supported by a bootstrap value > 85 .

Extended Data Figure 5 | Multiple sequence alignment of the deduced amino acid sequence of D53 with its homologues. D53 protein is predicted to contain an N-terminal domain, a D1 ATPase domain, an M domain and a D2 ATPase domain (<http://toolkit.tuebingen.mpg.de/hhpred>). The beginning and ending sites of each domain are indicated above the sequences. The predicted Walker A (P-loop) and Walker B motifs are shown in red boxes in the D1 domain and green boxes in the D2 domain, respectively. Note that the deletion

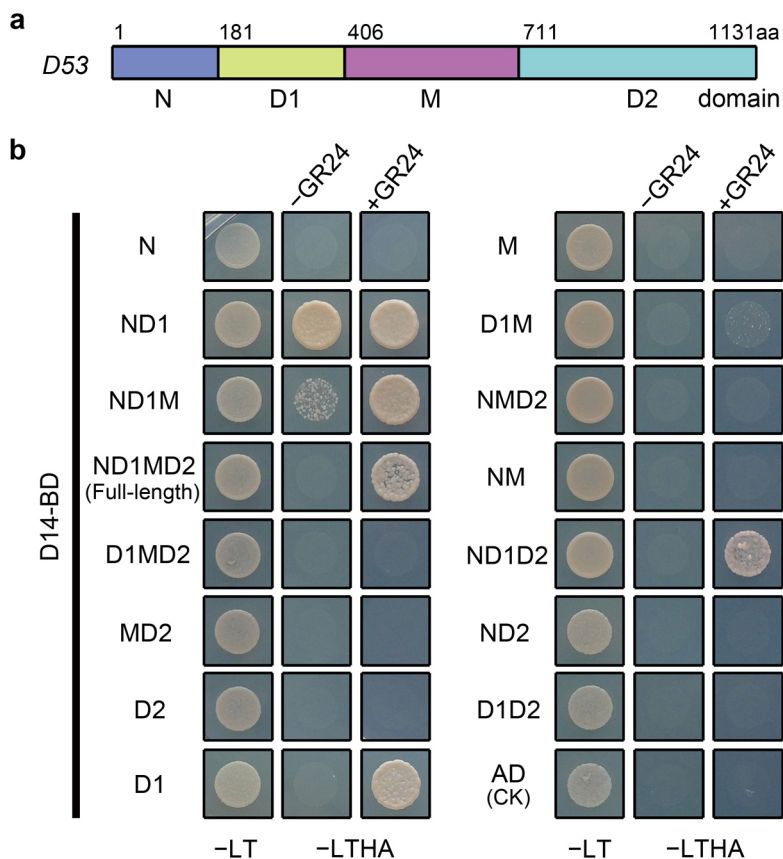
of five amino acids in the D2 domain of d53 protein overlaps with the GYVG loop in ClpC. The conserved putative EAR motif in D53 and ClpP-binding loop in ClpC are also shown. The sequences used for alignment are D53 (*Oryza sativa*, LOC_Os11g01330), D53-like (*Oryza sativa*, LOC_Os12g01360), SMXL6 (*Arabidopsis*, At1g07200), SMXL7 (*Arabidopsis*, At2g29970) and ClpC (*Bacillus subtilis*, GI: 16077154).



Extended Data Figure 6 | Histochemical staining of the *pD53::GUS* reporter gene and subcellular localization of D53 protein.

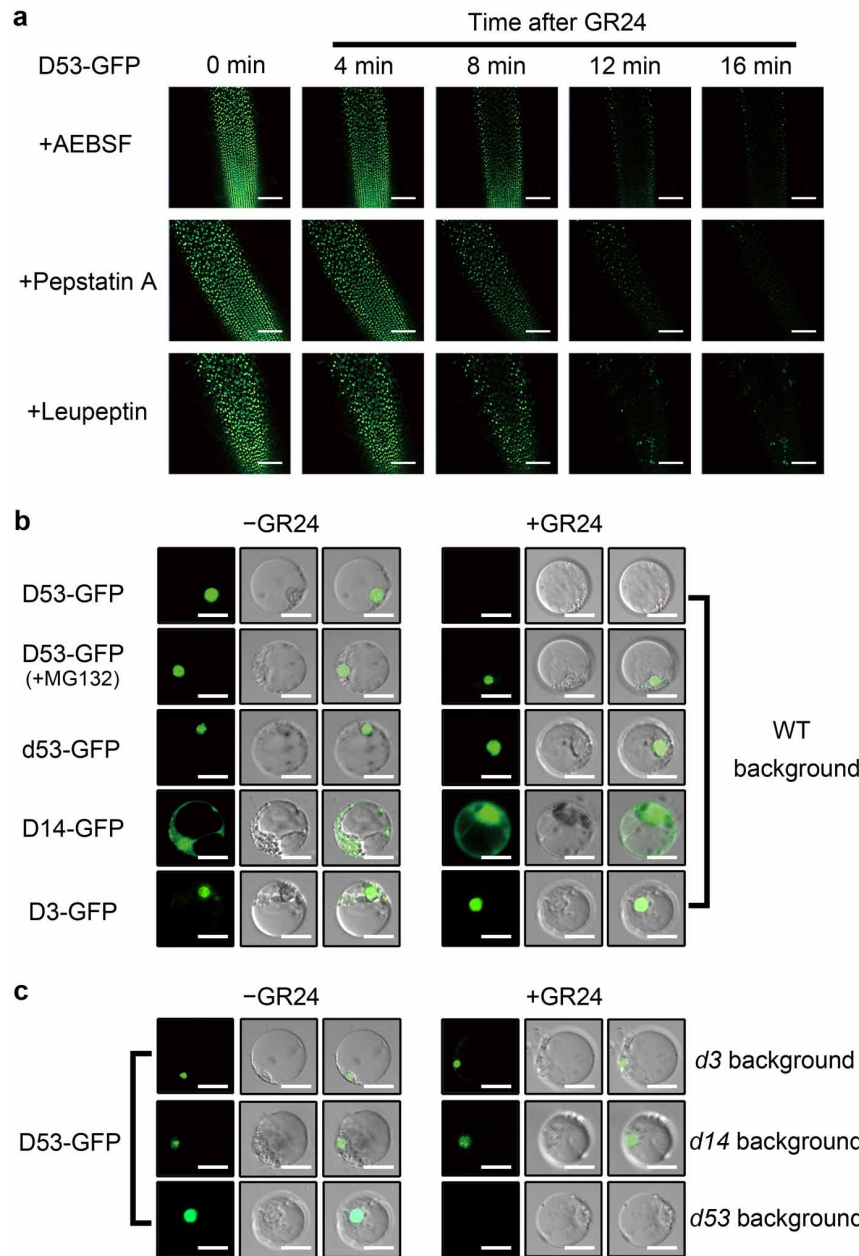
a–h, Histochemical staining of young root (**a**), shoot (**b**), leaf (**c**), leaf sheath (**d**), panicle (**e**), transverse section of the leaf sheath (**f**), stem (**g**) and node (**h**). Scale bars, 1 mm (**a, b, c, d, f, h**), 1 cm (**e**), 100 µm (**g**). **i–l,** Subcellular

localization of D53-GFP fusion protein in rice protoplast cells. A nuclear marker protein, OsMADS3, fused with mCherry, was used as a positive control. Scale bars, 5 µm. **m–p,** Confocal scanning images showing nuclear localization of the D53-GFP fusion protein in transgenic root cells. Scale bars, 100 µm.

**Extended Data Figure 7 | Mapping of the D14-binding domain of D53.**

a, Schematic structure of the D53 protein. Numbers indicate amino-acid (aa) residues. **b**, Y2H analysis showing interaction between full-length and various

domain deletion variants of D53 with D14 in the presence or absence of 5 μ M GR24. –LT, control medium (SD –Leu/-Trp); –LTHA, selective medium (SD –Leu/-Trp/-His/-Ade).

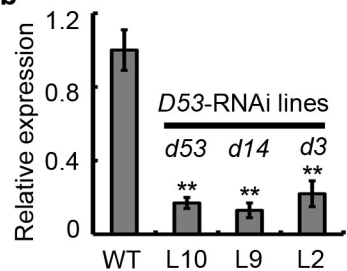
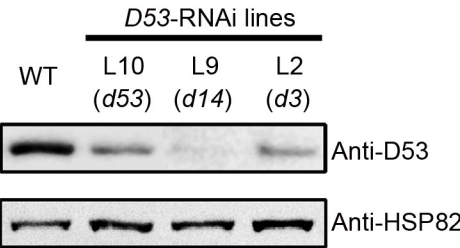
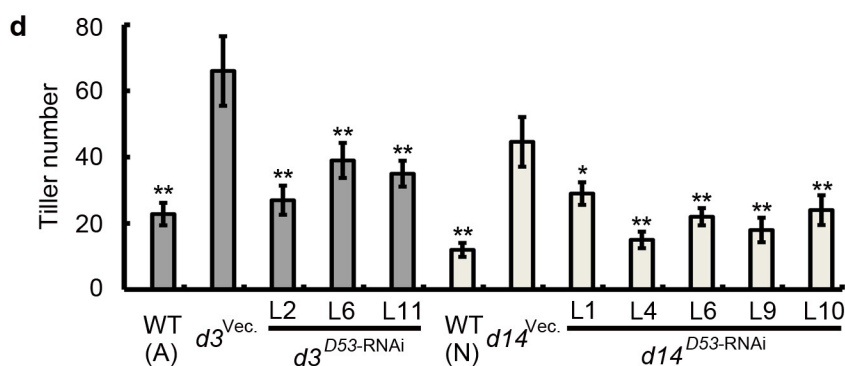

Extended Data Figure 8 | GR24 promotes D53 protein degradation.

a, Confocal scanning images showing that AEBSF, pepstatin A and leupeptin are not effective in blocking D53–GFP fusion protein degradation in transgenic seedlings treated with 5 μ M GR24. Scale bars, 100 μ m. **b**, Degradation of D53–GFP fusion protein but not D3–GFP or D14–GFP fusion proteins expressed in

rice protoplasts, in the presence of 5 μ M GR24. Pre-treatment with 40 μ M MG132 for 1 h before addition of GR24 effectively blocks D53–GFP degradation. **c**, D53–GFP is degraded in the *d53* mutant protoplasts in the presence of GR24, but not in *d3* or *d14* protoplasts. For **b** and **c**, each figure represents at least 50 cells observed. Scale bars, 10 μ m.

a

	Plant height (cm)	Diameter of 3 rd internode (mm)	Tiller number
WT (Norin 8)	107.2±1.4	4.69±0.11	16.9±3.1
<i>d53</i>	63.4±2.4	2.52±0.05	49.3±6.8
<i>d14</i>	61.5±2.1	2.47±0.19	51.3±5.5
<i>d14d53</i>	60.1±1.8	2.55±0.17	53.2±7.4
WT	91.6±2.1	4.39±0.29	18.3±2.3
<i>d53</i>	52.1±1.8	2.61±0.28	81.3±8.2
<i>d3</i>	39.8±2.1	1.52±0.15	101.4±11.2
<i>d3d53</i>	40.1±1.1	1.53±0.12	107.3±13.7

b**c****d**

Extended Data Figure 9 | *D53*-RNAi transgenic lines in *d3* and *d14* backgrounds. **a**, Comparison of plant height, diameter of the third internode and tiller number between wild type, *d53*, *d14*, *d3* and their double mutants. Values are mean ± s.d. ($n = 10$). **b**, **c**, qRT-PCR assay (**b**) and western blot analysis (**c**) showing that the endogenous level of *D53* messenger RNAs and proteins are downregulated in three representative *D53*-RNAi lines in *d53*, *d14* and *d3* mutant backgrounds, compared to wild-type control. Data are means ± s.d. ($n = 3$); significant difference determined by *t*-test (** $P < 0.01$). Anti-HSP82 was used as a loading control. **d**, Tiller number of representative

D53-RNAi transgenic lines in *d3* and *d14* mutant backgrounds at the heading stage. Each value represents the mean ± s.d. of six plants. L2, L6 and L11 represent three independent lines in *d3* background, and L1, L4, L6, L9 and L10 represent five independent lines in *d14* background. Akumuro (A) and Norin 8 (N) are the wild-type varieties correspond to *d3* and *d14* mutants, respectively. *d3*^{Vec.} and *d14*^{Vec.} transgenic lines were used as the controls. Asterisks represent significant difference compared with vector control determined by the *t*-test at * $P < 0.05$ and ** $P < 0.01$, respectively.